

## Image-potential band-gap narrowing at a metal/semiconductor interface

Ryotaro Arita,<sup>1</sup> Yoshiaki Tanida,<sup>2</sup> Kazuhiko Kuroki,<sup>3</sup> and Hideo Aoki<sup>1</sup>

<sup>1</sup>*Department of Physics, University of Tokyo, Hongo, Tokyo 113-0033, Japan*

<sup>2</sup>*Fujitsu Laboratories Ltd., 10-1, Morinosato-Wakamiya, Atsugi, Kanagawa 243-0197, Japan*

<sup>3</sup>*Department of Applied Physics and Chemistry, University of Electro-Communications, Chofu, Tokyo 182-8585, Japan*

(Received 26 July 2001; published 10 December 2001)

The *GW* approximation is used to systematically revisit the image-potential band-gap narrowing at metal/semiconductor interfaces proposed by Inkson in the 1970s. Here we have questioned how the narrowing as calculated from quasiparticle energy spectra for the jellium/Si interface depends on  $r_s$  of the jellium. The gap narrowing is found to only weakly depend on  $r_s$  (i.e., narrowing  $\approx 0.3$  eV even for a large  $r_s$  of 6). Hence we can turn to a smaller polarizability in the semiconductor side as an important factor in looking for larger narrowing.

DOI: 10.1103/PhysRevB.64.245112

PACS number(s): 73.30.+y, 73.40.Sx

### I. INTRODUCTION

Disrupted translational symmetry at surfaces and interfaces provides a potentially rich playing field for many-body effects. A seminal proposal was in fact made by Inkson back in the 1970s, who proposed that a metal-insulator transition can take place around the interface.<sup>1-5</sup> Classically, his argument is as follows. When a metal is placed on top of a semiconductor, an electron in the semiconductor feels an image potential, which is the interaction between the particle and its image charge in the metal. This leads to a downward bending of the conduction band bottom toward the interface,  $1/(4\epsilon z)$ , where  $\epsilon$  is the dielectric constant of the semiconductor and  $z$  is the distance from the interface. Similarly, the valence band top is bent upward by the same amount.

Quantum mechanically, this is described as follows.<sup>4</sup> The contribution of the correlation term to the self-energy of the electron in the semiconductor is similar [ $\sim -1/(4\epsilon z)$ ] for the conduction and valence bands. On the other hand, while the screened exchange term almost vanishes for the conduction band, it amounts to  $\sim 1/(2\epsilon z)$  for the valence band. As a result, while the conduction band bends downward as  $-1/(4\epsilon z)$ , the valence band bends upward as  $1/(4\epsilon z)$ . This kind of band bending can occur over short distances [ $z \sim \mathcal{O}(10 \text{ \AA})$ ], while the usual Schottky barrier occurs over much larger distances [ $z \sim \mathcal{O}(100-1000 \text{ \AA})$ ].

After the proposal of Inkson was made, various studies for the band-gap reduction or closure at metal/semiconductor(insulator) interfaces were performed theoretically and experimentally.<sup>6-9</sup> Recently, Murata *et al.*<sup>6</sup> have studied Ru(0001)/Al<sub>2</sub>O<sub>3</sub> and have observed the band-gap narrowing of Al<sub>2</sub>O<sub>3</sub>. Kiguchi *et al.*<sup>7</sup> have studied LiCl films on Cu(001) and have found that the 3*p* level of Cl shifts up to the Fermi level as the number of LiCl layers decreases.

As for the first principles many-body calculation, Charlesworth *et al.*<sup>9</sup> have calculated the quasiparticle electronic structure of Al/GaAs(110) and have shown the band-gap narrowing for the first time. The amount of the band-gap reduction turned out to be about 0.4 eV.

A big issue remains, however: which combination of metal and semiconductor will favor the local metal-insulator transition? As a first step toward such studies, we should

investigate how the band-gap reduction depends on the density of electrons (as represented by  $r_s$ ) in the metallic side, which governs the electron correlation in that side. The value of  $r_s$  in metals in fact extends over a wide range, 1.8–5.6, and the image-potential effect in metals with greater  $r_s$  is expected to be smaller than that for a smaller  $r_s = 2.1$ , a value corresponding to Al and assumed by Charlesworth *et al.*<sup>9</sup> If the band-gap narrowing still occurs significantly for metals with larger  $r_s$ , we can turn our attention to the semiconductor side in optimizing the local metal-insulator transition.

This is exactly the purpose of the present paper, i.e., to discuss the  $r_s$  dependence of the band-gap reduction quantitatively. Since  $r_s$  governs the dielectric response, the image-potential effect may well depend sensitively on  $r_s$ , which is why we have to look into the dependence from first principles. For that purpose we have to go beyond the usual local density functional approximation (LDA), since we are talking about the effects of screening. So here we adopt what is called the *GW* approximation, which is roughly the random-phase approximation (RPA)+LDA.

### II. MODEL

To focus on the problem described above, we can simplify the metallic side into the jellium model. On the other hand, we have to have an atomistic model for the semiconductor side, since we are questioning effects occurring on the length scale of a few atomic spacings on this side. So the model is depicted in Fig. 1. To facilitate the band calculation, we adopt a repeated-slab model (periodic boundary condition), in which the semiconductor slabs alternate with the jellium slabs. We calculate the band structure in the  $k_x$ - $k_y$  space.

When a semiconductor and a metal are put together, the Fermi energies in the metal and semiconductor have to be aligned in thermal equilibrium, which implies that some charges should flow across the interface, resulting in a charged region on the semiconductor side in general (in the absence of impurity levels in the semiconductor gap). This charge redistribution creates an electrostatic potential, and this bends the valence and conduction bands of the semiconductor, which become significant at distances  $z \sim \mathcal{O}(100-1000 \text{ \AA})$ . Since what we want to look at is the

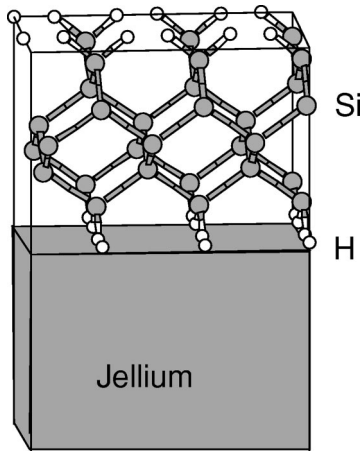


FIG. 1. The model studied in the present work. The slabs, each of which consists of Si layers terminated by H atoms, sandwich the jellium (metallic) region.

physics on the scale of  $O(10\sim 100 \text{ \AA})$ , we can neglect this bending (unless the charge rearrangement is substantial). In fact, Charlesworth *et al.*<sup>9</sup> have estimated the effect of the charge redistribution for Al/GaAs(110), where electrons flow from Al with a higher Fermi energy to the lower conduction band bottom in GaAs, and found the effect to be negligible. However, when there is large charge rearrangement, this one-body effect can become significant. Thus, to focus on the image-potential effect we have to exclude the one-body potential effect carefully. For this purpose, we set the Fermi energy of the metal inside the energy gap of the semiconductor (Fig. 2). As we shall show, such a situation is indeed realized if we take an appropriate value of  $r_s$  for the jellium model.

As for the semiconductor side, we have employed a slab, which consists of five layers of Si atoms stacked in the [001] direction. To eliminate complications arising from dangling bonds, the edges are terminated by hydrogen atoms. For the structure of the hydrogen-terminated surface, we assume for simplicity a nonreconstructed one [ $p(1\times 1)$ ]. With this assumption we have optimized the structure imposing mirror-

plane symmetries (along [100] and [010]) and an inversion + mirror symmetry ([001]). The hydrogen atoms are allowed to relax in any direction. The size of a supercell is  $7.18^2 \times 30.48 \text{ a.u.}^3$  along  $(x,y,z)$ , with the thickness of the jellium being 12.51 a.u.

The band-gap narrowing or closure in the semiconductor is probed here by identifying the character of the wave functions for various bands for the repeated slab model: by concentrating on the bands whose wave functions have their amplitudes primarily on the semiconducting side we can define the gap of the semiconductor.

### III. METHOD

Band-structure calculations are usually performed within the framework of the LDA. In this formalism, many-body effects are represented by the so-called exchange-correlation potential, which is a functional of the electron density. In practice, this potential is approximated as a function of the local density, and thus we have the LDA.

While the density-functional formalism is shown to be rigorous for the ground state<sup>10</sup> and LDA gives reliable information about the ground-state properties for various electron systems, it is well known that these approaches are not useful for excited states. In fact, the LDA usually underestimates the band gap of semiconductors and insulators. Moreover, the LDA cannot be applied to the cases where the electron density varies in space.

Still, LDA wave functions are usually good approximations to quasiparticle wave functions.<sup>11</sup> Since excitations can be described by many-body perturbation theory, it should be quite a good starting point to adopt the LDA wave functions as the basis for the many-body perturbation theory in determining the self-energy and spectrum of the quasiparticles.

For the calculation of the self-energy, various approximations have been developed. Among them, Hedin's *GW* approximation<sup>12,13</sup> often gives excellent quasiparticle energies in bulk semiconductors with a comparatively simple formalism.<sup>11,14</sup> The *GW* approximation essentially amounts to the RPA in the LDA formalism, so we have adopted this method to study the image-potential band-gap reduction.

#### A. LDA

So the first task in the present study is to perform an LDA calculation to obtain the eigen-wave-functions for the system described above. We adopt the exchange-correlation functional  $V_{xc}^{LDA}$  introduced by Perdew and Wang,<sup>15</sup> and eigen-wave-functions are expanded by plane waves up to a cutoff energy of 16 Ry. As for the atomic pseudopotentials, soft, norm-conserving pseudopotentials in a separable form<sup>16</sup> are employed. The atomic configurations and the corresponding electronic states in the ground states are obtained with the conjugate gradient scheme.<sup>17</sup>

#### B. Self-energy correction in the *GW* approximation

We then proceed to the *GW* approximation (GWA) calculation. The central idea of the GWA is to approximate the self-energy operator  $\Sigma$  by

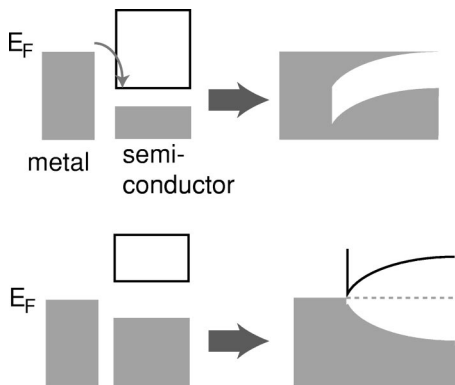


FIG. 2. Two cases where there is a charge transfer across the metal-semiconductor interface (top panel) or there is no charge redistributions with the Fermi energy of the metal lying within the gap of the semiconductor (bottom).

$$\Sigma(\mathbf{r}, \mathbf{r}'; \omega) = \frac{i}{2\pi} \int d\omega' G(\mathbf{r}, \mathbf{r}'; \omega + \omega') W(\mathbf{r}, \mathbf{r}'; \omega') e^{i\omega' \delta},$$

where  $\delta$  is an infinitesimal positive time and  $W$  is the screened Coulomb interaction,

$$W(\mathbf{r}, \mathbf{r}'; \omega) = \int d\mathbf{r}'' \frac{1}{\epsilon(\mathbf{r}'', \mathbf{r}'; \omega) |\mathbf{r} - \mathbf{r}''|},$$

where  $\epsilon$  is the dielectric function.

Recently, Rojas *et al.*<sup>18</sup> proposed a new implementation of GWA, the space-time approach, which is described in detail by Rieger *et al.*<sup>19</sup> The quasiparticle calculations can be performed either in reciprocal space as a function of the frequency or in real space as a function of the imaginary time, and the central idea in this method is to choose the representation that minimizes the computations required to evaluate the basic GWA quantities. This approach enables us to study larger systems.

The actual computational steps in this method are as follows. First, split the self-energy into a bare exchange part  $\Sigma^X$  and an energy-dependent correlation contribution  $\Sigma^C(E)$ . The former can be calculated from

$$\langle m\mathbf{k} | \Sigma^X | m\mathbf{k} \rangle = -\frac{4\pi}{V} \sum_v^{\text{occ}} \sum_{\mathbf{q}, \mathbf{G}} \frac{|M_{\mathbf{G}}^{vm}(\mathbf{k}, \mathbf{q})|^2}{|\mathbf{q} + \mathbf{G}|^2}.$$

Here  $\mathbf{G}$  is the reciprocal-lattice vector, and

$$M_{\mathbf{G}}^{vm}(\mathbf{k}, \mathbf{q}) = \int \Phi_{v, \mathbf{k}-\mathbf{q}}(\mathbf{r}) e^{-i(\mathbf{q}+\mathbf{G}) \cdot \mathbf{r}} \Phi_{m, \mathbf{k}}(\mathbf{r}) d\mathbf{r},$$

where  $\Phi_{v, \mathbf{k}-\mathbf{q}}$  is the wave function in the valence band of the semiconductor, while  $\Phi_{m, \mathbf{k}}$  is the wave function in the  $m$ th band.

To evaluate the energy-dependent self-energy  $\Sigma^C(E)$ , we first construct Green's function in real space and imaginary time,

$$G_{\text{LDA}} = \begin{cases} i \sum_{n\mathbf{k}}^{\text{occ}} \Phi_{n\mathbf{k}}(\mathbf{r}) \Phi_{n\mathbf{k}}^*(\mathbf{r}) \exp(\epsilon_{n\mathbf{k}} \tau), & \tau > 0 \\ -i \sum_{n\mathbf{k}}^{\text{unocc}} \Phi_{n\mathbf{k}}(\mathbf{r}) \Phi_{n\mathbf{k}}^*(\mathbf{r}) \exp(\epsilon_{n\mathbf{k}} \tau), & \tau < 0 \end{cases}$$

where  $\Phi_n$  and  $\epsilon_n$  are LDA wave functions and eigenvalues. Due to a rapid decay of the exponentials, the convergence against the cutoff in  $\sum_{n\mathbf{k}}^{\text{unocc}}$  is much better than that in the real frequency formalism.

Next, the RPA irreducible polarizability  $\chi^0(\mathbf{r}, \mathbf{r}'; i\tau)$  is calculated in real space and imaginary time, and Fourier-transformed to reciprocal space and imaginary energy. Then, the symmetrized Hermitian dielectric matrix<sup>20</sup>  $\tilde{\epsilon}_{\mathbf{G}, \mathbf{G}'}(\mathbf{k}, i\omega)$  is constructed, and inverted for each  $\mathbf{k}$  point.

Then the screened Coulomb interaction is calculated as

$$W_{\mathbf{G}\mathbf{G}'}(\mathbf{k}, i\omega) = \frac{4\pi}{|\mathbf{k} + \mathbf{G}| |\mathbf{k} + \mathbf{G}'|} \tilde{\epsilon}_{\mathbf{G}, \mathbf{G}'}(\mathbf{k}, i\omega)^{-1},$$

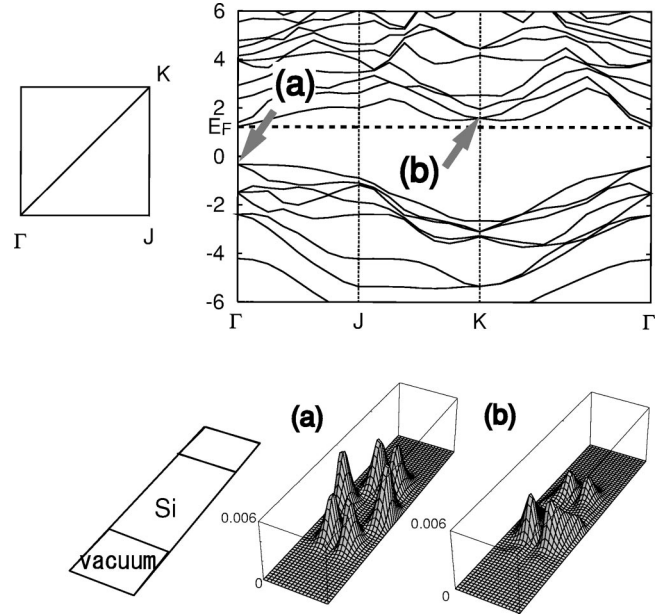


FIG. 3. The band structure of five Si layers terminated by hydrogen atoms in vacuum. The squared absolute value of the LDA wave functions at the valence top (a) and conduction bottom (b) are also shown.

and is Fourier-transformed to real space and imaginary time. The self-energy operator can be calculated as

$$\Sigma^C(\mathbf{r}, \mathbf{r}'; i\tau) = iG_{\text{LDA}}(\mathbf{r}, \mathbf{r}'; i\tau) W(\mathbf{r}, \mathbf{r}'; i\tau).$$

Finally, we evaluate the correlation contribution,  $\Sigma^C(i\tau) = \langle \mathbf{k}n | \Sigma^C | \mathbf{k}n \rangle$ . After this is Fourier-transformed to imaginary energy, we perform an analytic continuation onto the real energy axis with the Padé approximation.<sup>21</sup>

In the present study, we consider a  $6 \times 6 \times 24$  grid for the unit cell, and a  $6 \times 6$  grid for  $(k_x, k_y)$ . The time grid is spaced by  $\delta\tau = 0.3$  a.u. over the range of 13 a.u. We have taken up to 253 states to construct the Green's function.

## IV. RESULT

Let us move on to the results. The quasiparticle spectrum  $\epsilon^{\text{QP}}$  is obtained as

$$\epsilon^{\text{QP}} = \epsilon^{\text{LDA}} - V_{\text{xc}}^{\text{LDA}} + \Sigma^X + \Sigma^C.$$

In the following, we discuss the effect of the metallic layer for each term in  $\epsilon^{\text{QP}}$ .

### A. The LDA calculation

We first show the band structure and the (squared absolute value of) the wave functions obtained with LDA for  $r_s = \infty$ , i.e., no jellium (Fig. 3),  $r_s = 6$  (Fig. 4) and  $r_s = 4$  (Fig. 5), respectively. In the absence of the metal ( $r_s = \infty$ ), we can see that the valence band top is at  $\Gamma$ , while the conduction band bottom lies around  $K$  (and  $\Gamma$ ). Hereafter, we focus on the energy shifts of the valence band top around  $\Gamma$  and the conduction band bottom around  $K$  caused by the close contact with the jellium.

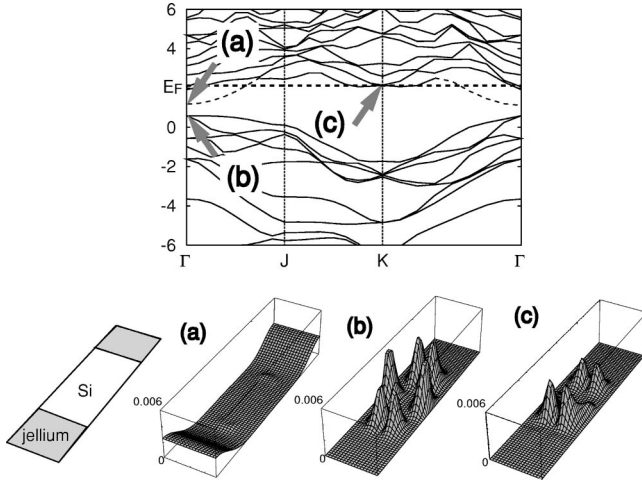


FIG. 4. A plot similar to Fig. 3, when the jellium with  $r_s=6$  is attached to the Si layer. The branch whose amplitude is localized in the jellium region is denoted by dotted lines.

When in vacuum the LDA band gap between  $K$  and  $\Gamma$  is 1.93 eV. When we introduce the jellium with  $r_s=6$  or 4, the Fermi level still lies between  $K$  and  $\Gamma$ , i.e., only a small amount of electrons flow from the jellium into the Si side, so the effect of the charge rearrangement is almost completely absent. For smaller values of  $r_s$ , on the other hand, we can show that electrons in the jellium do flow into the Si side, and the electronic band structure changes drastically. Thus we focus here on the case of  $r_s=6$  and 4.

For  $r_s=6$  (4), the band gap across  $\Gamma$  and  $K$  reduces to 1.85 (1.79) eV. The characteristics of the wave functions at these points are mainly Si and do not change, as we can see in Figs. 3–5. In addition, we notice that there is a state that emerges around  $\Gamma$  crossing the Fermi level for  $r_s=4,6$  (the bands represented by dotted lines in the figures). If we examine the character of wave functions on these branches in Figs. 4 and 5, they reside well within the metallic side, so we exclude them from our argument on the band-gap narrowing in the semiconductor side.

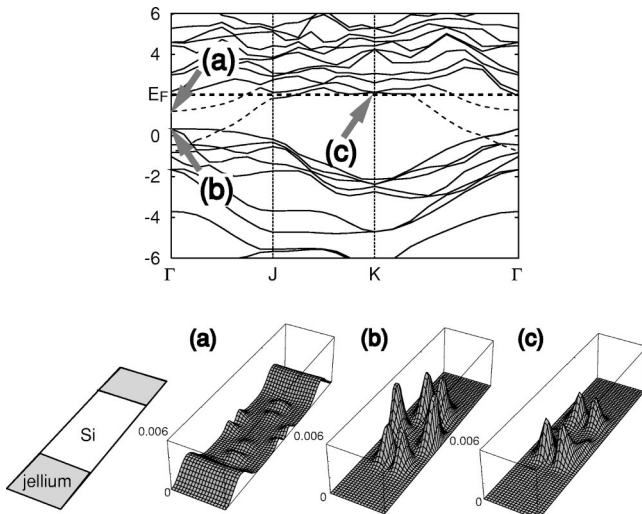


FIG. 5. A plot similar to Fig. 4, for  $r_s=4$ .

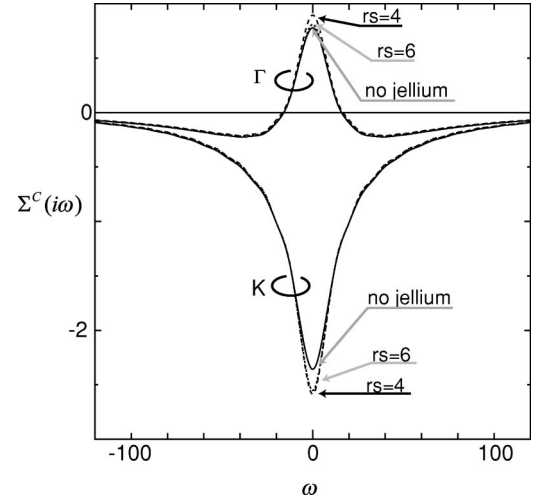


FIG. 6. The imaginary frequency dependence of the energy-dependent  $\Sigma^C$  at  $\Gamma$  and  $K$ . The dotted line is for  $r_s=4$ , the dashed line is for  $r_s=6$ , and the solid line is for  $r_s=\infty$ .

### B. $V_{XC}$ and the direct exchange term $\Sigma^X$

Now we are in a position to analyze the band-gap reduction term by term. Here we consider  $V_{XC}$  and the direct exchange term  $\Sigma^X$ , the energy-independent part of the  $GW$  correction to the LDA eigenenergy. The expectation value of the exchange-correlation potential is obtained by  $\langle V_{xc}^{LDA} \rangle \equiv \int |\Phi_{k,n}(\mathbf{r})|^2 V_{xc}^{LDA}(\mathbf{r}) d\mathbf{r}$ . We have found that  $V_{xc}^{LDA}(\mathbf{r})$  in the Si region has similar values for  $r_s=\infty, 6$ , and 4. Since the characters of the wave functions do not change as we have seen in Figs. 3–5, we can expect that  $\langle V_{xc}^{LDA} \rangle$  does not change significantly when we introduce the jellium in the Si system.

On the other hand, the value of the matrix elements between the metal wave functions and the semiconductor wave functions,  $M_{vc}^{vc}(\mathbf{k}, \mathbf{q})$ , which governs  $\Sigma^X$ , are small, since the states of jellium character and Si character are well separated in real space (see Figs. 4 and 5). Therefore, we can expect that  $\Sigma^X$  does not change significantly when we introduce the jellium. In fact,  $-V_{XC} + \Sigma^X$  at  $K$  is  $3.99 \rightarrow 4.00 \rightarrow 3.98$  in eV for  $r_s=\infty \rightarrow 6 \rightarrow 4$ , so the shift is negligible. At  $\Gamma$ ,  $-V_{XC} + \Sigma^X$  is  $-2.09 \rightarrow -2.00 \rightarrow -1.93$  in eV for  $r_s=\infty \rightarrow 6 \rightarrow 4$ .

### C. Energy-dependent $\Sigma^C$

Finally, let us discuss the correlation contribution,  $\Sigma^C$ . In Fig. 6, we show the imaginary frequency dependence of  $\Sigma^C$  at  $\Gamma$  and  $K$ .

We have then performed an analytic continuation onto the real energy axis with the Padé approximation.<sup>21</sup> In Fig. 7, we show the real frequency dependence of  $\Sigma^C$ . We can see that there is an almost linear dependence on  $\omega$ .

When  $\Sigma^C$  is linear for small  $\omega$ , the  $GW$  correction to the LDA spectrum reduces to

$$\Delta = \frac{1}{Z_{nk}} \langle \Phi_{nk} | \Sigma^C(\epsilon_{nk}^{LDA}) + \Sigma^X - V_{XC} | \Phi_{nk} \rangle,$$

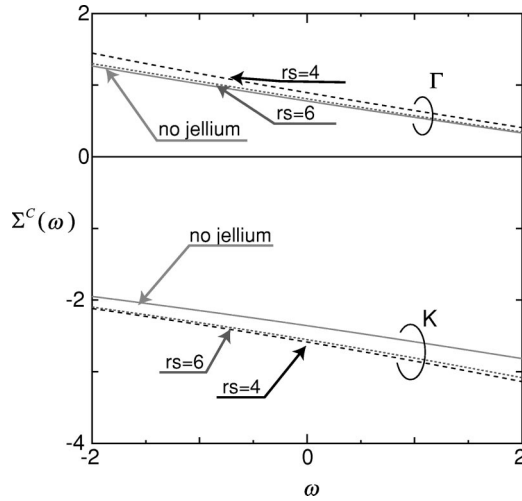


FIG. 7. The real frequency dependence of the  $\Sigma^C$  at  $\Gamma$  and  $K$ . The dotted line is for  $r_s=4$ , the dashed line is for  $r_s=6$ , and the solid line is for  $r_s=\infty$ .

where

$$Z_{nk} = 1 - \frac{d}{d\omega} \langle \Phi_{nk} | \Sigma^C(\omega) | \Phi_{nk} \rangle \Big|_{\omega = \epsilon_{nk}^{\text{LDA}}}.$$

From Fig. 7, we can see that  $Z_{nk} = -0.2$  to  $-0.3$ . At  $\Gamma$ ,  $\Delta$  is estimated to be  $-0.75 \rightarrow -0.60 \rightarrow -0.44$  in eV for  $r_s = \infty \rightarrow 6 \rightarrow 4$ . At  $K$ ,  $\Delta$  is  $1.28 \rightarrow 1.15 \rightarrow 1.09$  in eV. Thus the band-gap reduction due to the presence of the jellium amounts to as large as  $\approx 0.3$  eV for  $r_s=6$  and  $\approx 0.5$  eV for  $r_s=4$ .

## V. DISCUSSIONS

To summarize, we have studied, with the *GW* approximation and a character-resolved band analysis, the image-potential band-gap narrowing at a metal/semiconductor interface by calculating the quasiparticle energy spectrum of the jellium/Si interface. For the values of  $r_s=4-6$  of jellium studied here the electrons or holes do not flow from the metallic to semiconducting side, i.e., the Fermi energy of the jellium lies within the energy gap of Si, so the one-body effect due to the charge redistribution is absent. We have found that a significant band-gap narrowing of  $\approx 0.3$  eV occurs for  $r_s$  as large as 6.

So we can concentrate on the semiconducting side to realize larger gap-narrowing effects or a local metal-insulator transition. If the dielectric constant of the semiconductor is small, the image-potential effect will become stronger, so that we may expect larger band-gap narrowing. However, the system with a small dielectric function usually occurs in materials with a large band gap, so that the realization of the band-gap closure becomes a trade-off. Furthermore, the energy gap of the semiconducting layer may depend on the surface structure (e.g., whether it is terminated by hydrogen atoms or dangling bonds form dimers, etc.), and their effect is also nontrivial. These are interesting future problems.

Finally, while the band-gap narrowing or closure is of a fundamental interest in its own right, we can further raise a very strong motivation for considering a metallized semiconductor surface. There is a long history<sup>22</sup> of proposals for superconductivity in conducting systems in close contact with polarizable media. Little<sup>23</sup> proposed this for one-dimensional systems, and then Ginzburg<sup>24</sup> extended this to two-dimensional systems. Allender, Bray, and Bardeen<sup>25</sup> studied this in detail, with metal-semiconductor structures in mind, which was subsequently criticized by Inkson and Anderson.<sup>26</sup> A summary of the situation by Zharkov<sup>22</sup> is that while the criticism is correct for the usual form for the dielectric function, the situation may be resurrected for unusual dielectric functions. The background to all this is that for the polarizable-medium-mediated superconductivity, the conduction layer should be very strongly coupled to the semiconducting layer, ideally with strong chemical bonds such as covalent ones. Therefore the metallized semiconductor surface, with the band-closure mechanism, should be one ideal realization of this.

## ACKNOWLEDGMENTS

One of the authors (K.K.) is indebted to Y. Murata for arousing his interest in surface studies. H.A. wishes to thank J.C. Inkson for illuminating discussions. Thanks are also due to M. Tsukada, A. Koma, and M. Kiguchi for discussions. The LDA calculation was performed with TAPP (Tokyo Ab initio Program Package); R.A. would like to thank S. Koizumi for technical advice. The numerical calculation was performed with SR8000 in ISSP, University of Tokyo. This work is in part funded by a Grant-in-Aid for Scientific Research from Ministry of Education of Japan.

<sup>1</sup>J.C. Inkson, *Surf. Sci.* **28**, 69 (1971).

<sup>2</sup>J.C. Inkson, *J. Phys. C* **4**, 591 (1971).

<sup>3</sup>J.C. Inkson, *J. Phys. C* **5**, 2599 (1972).

<sup>4</sup>J.C. Inkson, *J. Phys. C* **6**, 1350 (1973).

<sup>5</sup>P.W. Anderson in *Elementary Excitation in Solids, Molecules and Atoms*, edited by J.A. Devreese, A.B. Kunz, and T.C. Collins (Plenum, New York, 1974), Part A, p. 1.

<sup>6</sup>Y. Murata *et al.* (unpublished).

<sup>7</sup>M. Kiguchi *et al.* (unpublished).

<sup>8</sup>A. Okiji and H. Kasai [*Surf. Sci.* **86**, 529 (1979)] have theoret-

cally studied the Mott gap closure at an interface in the Hubbard model.

<sup>9</sup>J.P.A. Charlesworth, R.W. Godby, and R.J. Needs, *Phys. Rev. Lett.* **70**, 1685 (1993).

<sup>10</sup>P. Hohenberg and W. Kohn, *Phys. Rev.* **140**, A1133 (1965).

<sup>11</sup>W.G. Aulbur, L. Jönsson, and J.W. Wilkins, in *Solid State Physics*, edited by H. Ehrenreich, F. Seitz, and D. Turnbull (Academic Press, New York, 2000), Vol. 54, p. 1.

<sup>12</sup>L. Hedin, *Phys. Rev.* **139**, A796 (1969).

<sup>13</sup>L. Hedin and S. Lundqvist, in *Solid State Physics*, edited by H.

- Ehrenreich, F. Seitz, and D. Turnbull (Academic Press, New York, 1969), Vol. 23, p. 1.
- <sup>14</sup>F. Aryasetiawan and O. Gunnarsson, Rep. Prog. Phys. **61**, 237 (1998).
- <sup>15</sup>J.P. Perdew and Y. Wang, Phys. Rev. B **45**, 13 244 (1992).
- <sup>16</sup>N. Troullier and J.L. Martins, Phys. Rev. B **41**, 7892 (1990).
- <sup>17</sup>J. Yamauchi, M. Tsukada, S. Watanabe, and O. Sugino, Phys. Rev. B **54**, 5586 (1996).
- <sup>18</sup>H.N. Rojas, R.W. Godby, and R.J. Needs, Phys. Rev. Lett. **74**, 1827 (1995).
- <sup>19</sup>M.M. Rieger, L. Steinbeck, I.D. White, H.N. Rojas, and R.W. Godby, Comput. Phys. Commun. **117**, 211 (1999).
- <sup>20</sup>S. Baroni and R. Resta, Phys. Rev. B **33**, 7017 (1986).
- <sup>21</sup>H.J. Vidberg and J.W. Serene, J. Low Temp. Phys. **29**, 179 (1977).
- <sup>22</sup>G.F. Zharkov, in *High-Temperature Superconductivity*, edited by V.L. Ginzburg and D.A. Kirzhnits (New York Consultants Bureau, New York, 1982).
- <sup>23</sup>W.A. Little, Phys. Rev. **134**, 1416 (1964).
- <sup>24</sup>V.L. Ginzburg, Zh. Éksp. Teor. Fiz. **46** 397 (1964) [Sov. Phys. JETP **19**, 269 (1964)].
- <sup>25</sup>D. Allender, J. Bray, and J. Bardeen, Phys. Rev. B **7**, 1020 (1973); **8**, 4433 (1973).
- <sup>26</sup>J.C. Inkson and P.W. Anderson, Phys. Rev. B **8**, 4429 (1973).